Virologica Sinica 40 (2025) 451–461

Contents lists available at ScienceDirect

Virologica Sinica

journal homepage: www.keaipublishing.com/en/journals/virologica-sinica
www.virosin.org

Research Article

Severe enterovirus A71 infection is associated with dysfunction of T cell immune response and alleviated by Astragaloside A

Chong Wang [a], Muhan Huang [a], Bingyu Guo [a], Xi Zhou [a,b], Zongqiang Cui [a,b,*], Yi Xu [c,*], Yujie Ren [a,b,*]

[a] State Key Laboratory of Virology and Biosafety, Wuhan Institute of Virology, Center for Biosafety Mega-Science, Chinese Academy of Sciences, Wuhan 430071, China
[b] University of Chinese Academy of Sciences, Beijing 100049, China
[c] Department of Infectious Disease, Women and Children's Medical Center, Affiliated to Guangzhou Medical University, Guangzhou 510623, China

ARTICLE INFO

Keywords:
Enterovirus A71 (EV-A71)
T-cell immunity
hand-foot-and-mouth disease (HFMD)
Astragaloside A
Immunotherapeutic strategy

ABSTRACT

Enterovirus A71 (EV-A71) is the major causative pathogen for severe hand-foot-mouth disease (HFMD), a predominantly childhood-associated communicable disease. The mechanisms that children manifest severe disease progression while adults typically exhibit milder or asymptomatic infections remain incompletely characterized, which hinders the development of effective therapy against this disease. Herein, using the newborn mouse model of EV-A71 infection, we uncovered that the underdevelopment of T cells closely associated with the severity of EV-A71 infection, and EV-A71 infection dramatically impaired T-cell immune response. Moreover, the dysfunction of T-cell immunity contributes to the pathogenesis of EV-A71 infection, as the loss of T cells made neonatal mice highly vulnerable to EV-A71 infection. To further assess the relationship between T-cell immunity and HFMD, we enrolled a cohort of 145 pediatric patients with laboratory-confirmed EV-A71 infection and found that the compromised T-cell immune response is associated with the severity of EV-A71-caused HFMD in these children. Furthermore, we found that the treatment of newborn mice with Astragaloside A, a saponin from the medicinal herb *Astragalus membranaceus*, showed potent *in vivo* therapeutic efficacy against EV-A71 infection in a T-cell-dependent manner. In conclusion, these findings uncover the interaction between EV-A71 infection and T-cell immunity, provide novel insights onto the physiological impacts of T cells on the pathogenesis of EV-A71 infection and HFMD, and find a promising immunotherapeutic strategy to treat this viral disease.

INTRODUCTION

Enteroviruses are a large group of non-enveloped, positive-sense and single-stranded RNA viruses belonging to the genus *Enterovirus* of the family *Picornaviridae*. Enteroviruses include numerous important human pathogens such as poliovirus, enterovirus A71 (EV-A71), coxsackieviruses, and echoviruses, and cause approximately 3 billion human infections per year in the world. The symptoms caused by enteroviral infections range from relatively mild conditions like upper respiratory illness and common cold to severe or even lethal outcomes such as severe hand-foot-and-mouth disease (HFMD), aseptic meningitis, encephalitis, myocarditis, neonatal sepsis-like disease, and poliomyelitis (Pallansch, 2007).

HFMD is a common pediatric infectious disease caused by infections with EV-A71 and some other enteroviruses including coxsackieviruses A16 (CV-A16), A6 (CV-A6), etc. There are millions of HFMD cases in children under 5 years old globally every year (Chan et al., 2000; Fioravanti, 2012; Ho et al., 1999; Tan et al., 2011). Although the symptoms of HFMD are usually moderate, this viral disease is highly contagious and spreads quickly at schools and kindergartens. Neurotropic EV-A71 is a major causative pathogen for HFMD, and EV-A71 infection is more frequently associated with severe central-nervous-system complications in HFMD and thereby is the major cause of fatalities in HFMD (Huang et al., 1999; Solomon et al., 2010). Thus, EV-A71 is considered as the most virulent pathogen within HFMD-causing enteroviruses and a serious threat to the health of children across the globe. Thus far, there is

* Corresponding authors.
E-mail addresses: renyujie@wh.iov.cn (Y. Ren), xuyi70@163.com (Y. Xu), czq@wh.iov.cn (Z. Cui).

https://doi.org/10.1016/j.virs.2025.05.010
Received 25 January 2025; Accepted 26 May 2025
Available online 29 May 2025

no effective antiviral drug or therapy available to specifically treat EV-A71 infection and HFMD.

Although EV-A71 infection and HFMD can occur in both children and adults, adult infection of this virus is usually asymptomatic, while severe symptoms are normally observed in children at preschool ages (Deng et al., 2011; Solomon et al., 2010; Zhu et al., 2015). Compared with adults, young children have less developed cellular immunity that is pivotal for controlling viral infection (Carsetti et al., 2020; Olin et al., 2018; Simon et al., 2015). Besides, a number of clinical observations have suggested the correlation between compromised cellular immunity and severe symptoms of enterovirus 71 (EV71) infection (Chang et al., 2006, 2008; Yang et al., 2001). However, the relationship between EV-A71 infection and T cells as well as the physiological impacts of T cell immune response on severe EV-A71 infection and HFMD are still poorly understood, which hinders the development of effective therapeutic strategy for HFMD.

In this study, using the newborn mouse model of EV-A71 infection, we uncovered that the underdevelopment of T cells, but not macrophages, dendritic cells (DCs), or B cells, was closely associated with the severity of EV-A71 infection. And EV-A71 infection dramatically impaired T cell immune response in newborn mice. Besides, the dysfunction of T cell immune response contributes to the pathogenesis of EV-A71 infection, which was further supported by our cohort study involving 145 pediatric patients with laboratory-confirmed EV-A71 infection and different symptoms. Furthermore, after revealing the relationship between T-cell immune response and the severity of EV-A71 infection and HFMD, we aimed to find an immunotherapy that can boost T cell immune response to treat EV-A71 infection. We found that the treatment of newborn mice with Astragaloside A (AGS-A), the primary saponin extracted from the traditional Chinese medicinal herb *Astragalus membranaceus* (Auyeung et al., 2016), effectively rescued the EV-A71-caused impairment of T cell immune response, activated T cells, and showed potent *in vivo* therapeutic efficacy against EV-A71 infection in a T-cell-dependent manner, while AGS-A treatment showed no direct antiviral effect in T-cell-deficient mice.

RESULTS

T cell development in newborn mice was associated with the severity of EV-A71 infection

We infected 1-, 3-, 7- or 14-day-old Institute of Cancer Research (ICR) mice with 1×10^7 PFU of EV-A71 by intraperitoneal (i.p.) injection (Fig. 1A). Our data showed that the 1- and 3-day-old mice developed to clinical symptoms from 5 d.p.i. and the mortality rates of the 1- and 3-day-old mice were 90% and 70%, respectively. Moreover, although the 7-day-old mice had post-inoculation symptoms, their mortality rate was 40%. Of note, all the 14-day-old mice survived without any symptoms after infection (Fig. 1B and Supplementary Fig. S1A). In addition, the viral loads in the spleen, muscle, and brain tissues of EV-A71-infected 3-day-old mice were significantly higher compared to that in EV-A71-infected 14-day-old mice (Supplementary Fig. S1B).

To examine the status of cellular immunity, especially T cells, in neonates of different ages, we examined the percentages of $CD3^+$ total T cells, $CD3^+CD4^+$ helper T cells, $CD3^+CD8^+$ T cells, $CD11b^+$ macrophages and $CD11c^+$ dendritic cells (DCs) in the spleen and TCR-β^+ T cells in the thymus of naive mice by flow cytometry on days 1, 3, 7 and 14 after birth. As shown in Fig. 1C–E, the percentages of $CD3^+$ T cells, $CD3^+CD4^+$ T cells and $CD3^+CD8^+$ T cells displayed the upward trend along with age. On the other hand, the percentage of macrophages in spleen decreased along with age (Supplementary Fig. S2A), while the percentages of $CD11c^+$ DCs and $CD19^+$ B cells in spleen and TCR-β^+ T cells in the thymus had no significant difference among each age group (Supplementary Fig. S2B–D). Our findings indicate that T cell development is closely associated with age in newborn mice.

Therefore, our findings suggest that the underdevelopment of T cells is correlated to the severity of EV-A71 infection in neonatal mice.

The dysfunction of T-cell immune response contributes to the pathogenesis of EV-A71 infection in newborn mice

To examine the roles of T cells on the severity of EV-A71 infection *in vivo*, we examined the status of T cells in 3- and 14-day-old mice infected with EV-A71 at 1, 3, 5, and 7 d.p.i. We chose 7 d.p.i. as the last time-point because the 3-day-old mice began to succumb to EV-A71 infection at that time (Fig. 1B). Our data showed that EV-A71 infection dramatically decreased the percentages of total T cells, $CD4^+$ T cells, and $CD8^+$ T cells in the spleen of the 3-day-old mice (Fig. 2A and B). On the other hand, for the 14-day-old mice, the percentages of total T cells, $CD4^+$ T cells, and $CD8^+$ T cells showed no significant difference between EV-A71-infected and non-infected groups (Fig. 2C and D). These results indicate that EV-A71 infection impaired the immune response of T cells in newborn (3-day-old) mice, which probably contribute to the disease severity of EV-A71 infection.

To further assess the roles of T cells in the pathogenesis of EV-A71 infection, we used BALB/c-nu$^{-/-}$ mice that lack thymus for T cell development. As expected, BALB/c-nu$^{-/-}$ mice had almost no T cells (Fig. 3A–D), while the B cells, $CD11b^+$ macrophages, and $CD11c^+$ DCs in these immunocompromised mice were not affected (Supplementary Fig. S3A–D). 10-day-old BALB/c-nu$^{-/-}$ mice and WT BALB/c mice were i.p. infected with 1×10^7 PFU/ml EV-A71. Our data showed that BALB/c-nu$^{-/-}$ mice began to succumb to EV-A71 infection from 8 d.p.i. and reached 100% mortality at 10 d.p.i., while the body weights of these mice began to decrease at 7 d.p.i. (Fig. 3E–G). In contrast, 80% of WT BALB/c mice survived the lethal viral challenge, while their body weights continued to increase and appeared normal compared with those in non-infected group. Moreover, both BALB/c-nu$^{-/-}$ and WT BALB/c mice began to have clinical symptoms at 4 d.p.i. (Fig. 3F), while BALB/c-nu$^{-/-}$ mice died quickly and WT BALB/c mice began to recover from 10 d.p.i. (Fig. 3G). Therefore, the loss of T cells made neonatal mice vulnerable to EV-A71 infection.

Together, our findings show that EV-A71 infection can impair T cell immune response, and the dysfunction of T cell immune response is associated with the pathogenesis of EV-A71 infection in newborn mice.

Cohort study revealed that the T-cell immune response is associated with the severity of HFMD cases caused by EV-A71 infection

It would be intriguing to find out whether the immune response of T cells in severe HFMD cases of pediatric patients is the same or similar with our observations in the newborn mouse model of EV-A71 infection. For this purpose, we enrolled a cohort of 145 pediatric patients with laboratory-confirmed EV-A71 infection at Guangzhou Women and Children's Medical Center. Among these patients, 61 children were diagnosed as severe symptoms, and 84 children were diagnosed as mild symptoms according to the Diagnosis and Treatment Protocol for HFMD published by the National Health Commission of China (2018 Edition) (http://www.nhc.gov.cn/cms-search/xxgk/getManuscriptXxgk.htm?id=5db274d8697a41ea84e88eedd8bf8f63). The clinical data of the 145 patients were shown in Supplementary Table S1. There was no significant difference in age between the severe and mild groups (Fig. 4A), and the gender of the two groups were matched (Fig. 4B). Our data showed that the numbers of T cells, including $CD45^+CD3^+$ total T cells,

$CD45^+CD3^+CD4^+$ T cells, $CD45^+$ $CD3^+CD8^+$ T cells, as well as NK cells in severe pediatric patients were significantly lower than those in the mild cases (Fig. 4C–F). On the other hand, the number of $CD45^+CD19^+$ B cells between the severe and mild groups showed no significant difference (Fig. 4G). These results show that the compromised immune response of T cells is associated with the severity of EV-A71-caused HFMDs in children, consistent with the experimental data obtained in the newborn mouse model of EV-A71 infection.

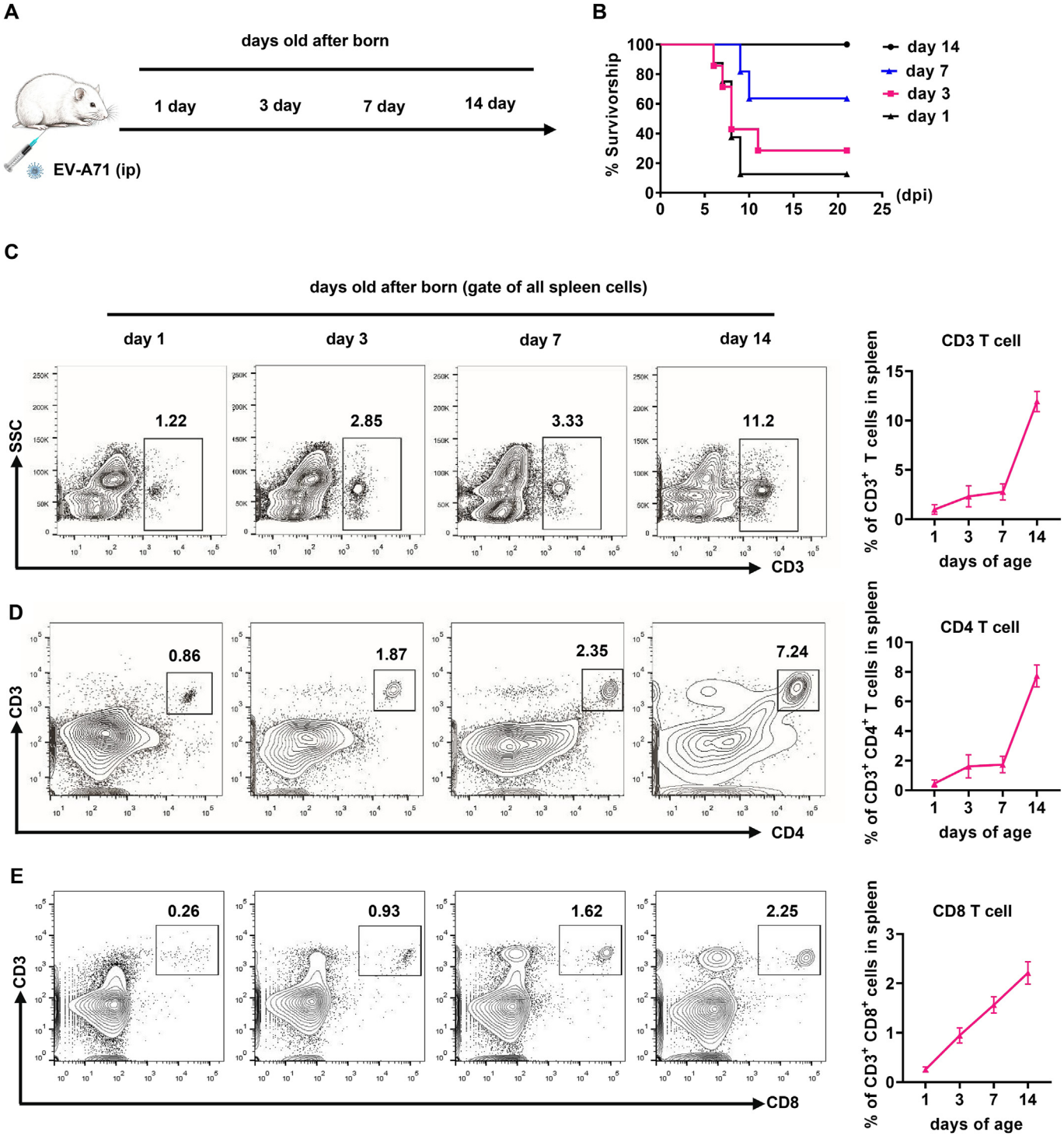

Fig. 1. T cell development in newborn mice was associated with the severity of enterovirus 71 (EV71) infection. The 1-, 3-, 7- or 14-day-old ICR mice were infected with enterovirus A71 (EV-A71) at 1×10^7 PFU **(A)**, the survival rates for mice in indicated groups during the 21-day period are shown by curves (**B**), (n = 10 for each group). Representative contour plots showed the percentages of $CD3^+$ T (**C**), $CD3^+CD4^+$ T (**D**) and $CD3^+CD8^+$ T cells (**E**) in the spleens of 1-, 3-, 7- or 14-day-old ICR mice (left). The curve diagram described the trend of T cells in spleens of 1-, 3-, 7- or 14-day-old ICR mice (right), (n = 3). Data are representative of three independent experiments. Graph shows mean ± SEM.

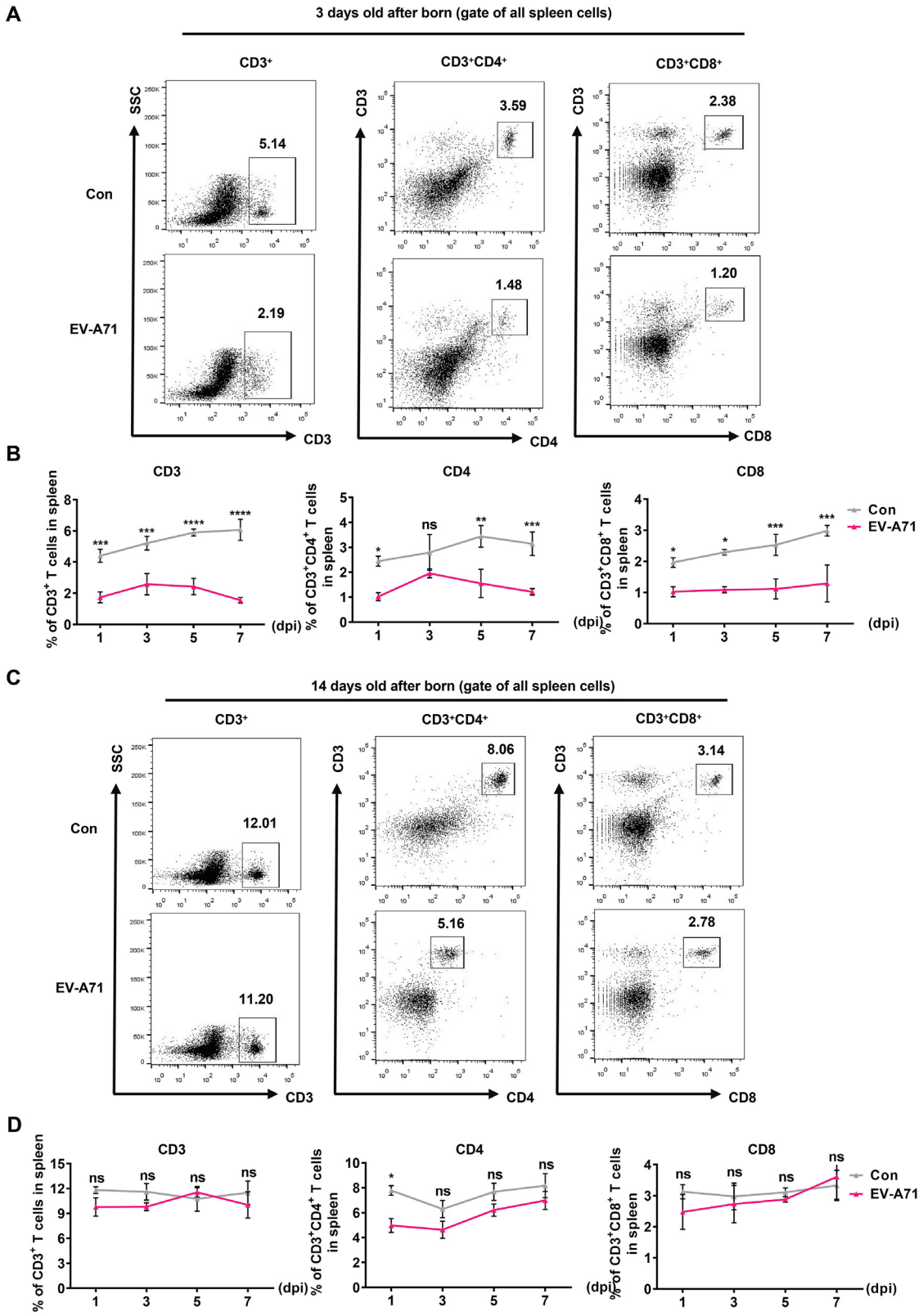

Fig. 2. EV-A71 infection impaired T-cell immune response in 3-day-old newborn mice. The 3-day-old and 14-day-old ICR mice were i.p. injected with 10^7 PFU of EV-A71 and splenocytes were analyzed every other day from 1 to 7 d.p.i. with flow cytometry. Representative scatter plots show the percentage of $CD3^+$ T cells, $CD3^+CD4^+$ T cells and $CD3^+CD8^+$ T cells in spleen of 3-day-old mice (**A**) or 14-day-old mice (**C**) at 5 dpi after EV-A71 infection. The curve diagram described the trend of $CD3^+$ T, $CD3^+CD4^+$ T cells and $CD3^+CD8^+$ T cells in 3-day-old (**B**) or 14-day-old (**D**) mice challenged with EV-A71 or non-infected (control) from 1 to 7 d.p.i. The bar charts illustrate the percentage of $CD3^+$ T, $CD3^+CD4^+$ T cells and $CD3^+CD8^+$ T cells in 3-day-old (**B**) or 14-day-old (**D**) mice at 3, 5 and 7 d.p.i. (n = 3 for control group and n = 5 for infection group). Data are representative of three independent experiments. Graph shows mean ± SEM, n = 3 for each group. *P* values were calculated via ANOVA. $^*P < 0.05$, $^{**}P < 0.05$, $^{***}P < 0.001$, and $^{****}P < 0.0001$, ns, no significance.

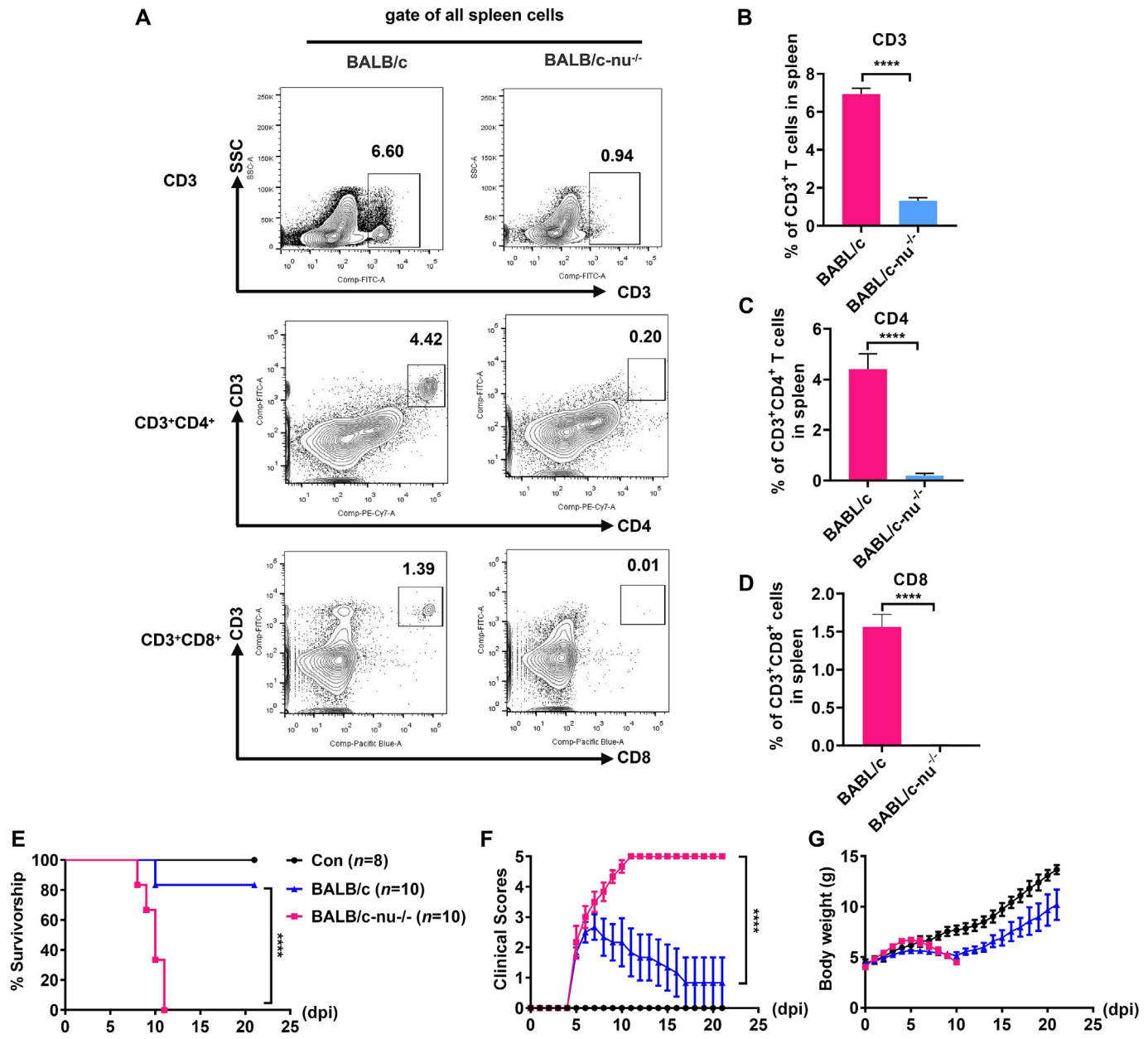

Fig. 3. The dysfunction of T-cell immune response contributes to the pathogenesis of EV-A71 infection in newborn mice. Representative scatter plots showed the percentages of $CD3^+$ T cells, $CD3^+CD4^+$ T cells and $CD3^+CD8^+$ T cells in spleen of WT BALB/c mice and T-cell-deficient mice (BALB/c-$nu^{-/-}$ mice) (**A**). The bar charts illustrate the percentage of $CD3^+$ T cells, $CD3^+CD4^+$ T cells and $CD3^+CD8^+$ T cells in spleen of BALB/c-$nu^{-/-}$ mice and WT BALB/c mice (**B**–**D**). (n = 3 for each group). 10-day-old BALB/c-$nu^{-/-}$ mice (n = 10) and WT BALB/c mice (n = 10) were i.p. infected with 1×10^7 PFU EV-A71, n = 3 for non-infected (control) group. The survival distribution for BALB/c-$nu^{-/-}$ and WT mice with lethal EV-A71 challenge during the 21-day period was shown by curves (**E**). Curves described the clinical scores of BALB/c-$nu^{-/-}$ and WT mice with lethal EV71 challenge (**F**). The average percentages of body weight changes were monitored between BALB/c-$nu^{-/-}$ and WT mice during the 21-day period is shown by curves (**G**). Data are representative of three independent experiments. Graph shows mean ± SEM. *P* values were calculated via ANOVA. ****$P < 0.0001$.

AGS-A treatment protected from lethal EV-A71 infection in a T-cell-dependent manner

After finding that the compromised T-cell immune response contributes to the pathogenesis of EV-A71 infection both in pediatric patients and animal models, the intriguing question is that whether enhancing T-cell immune response has any therapeutic potential to treat EV-A71 infection. AGS-A is a saponin extracted from *Astragalus membranaceus*. To assess the therapeutic potential of AGS-A on EV-A71 infection, we treated 5-day-old ICR mice with AGS-A via i.p. administration at a dose of 10 mg/kg 2 h after EV-A71 challenge, followed by treatment twice a day for 6 days. The mice in the vehicle group (control) began to succumb to EV-A71 infection from 8 d.p.i., and reached 50% mortality at 10 d.p.i. In contrast, 80% of the mice in the AGS-A therapeutic group survived the viral challenge (Fig. 5A). Consistently, we observed significant differences of body weights and clinical scores between the therapeutic and control groups (Supplementary Fig. S4A–C). In addition, the viral RNA accumulations of EV-A71 in muscle, spleen, and brain tissues were significantly reduced in the AGS-A therapeutic group compared with those in the control group at both 3 and 5 d.p.i. (Supplementary Fig. S4D). Moreover, we examined the therapeutic effects of AGS-A in EV-A71-infected mice at 12 h after viral challenge and obtained the similar

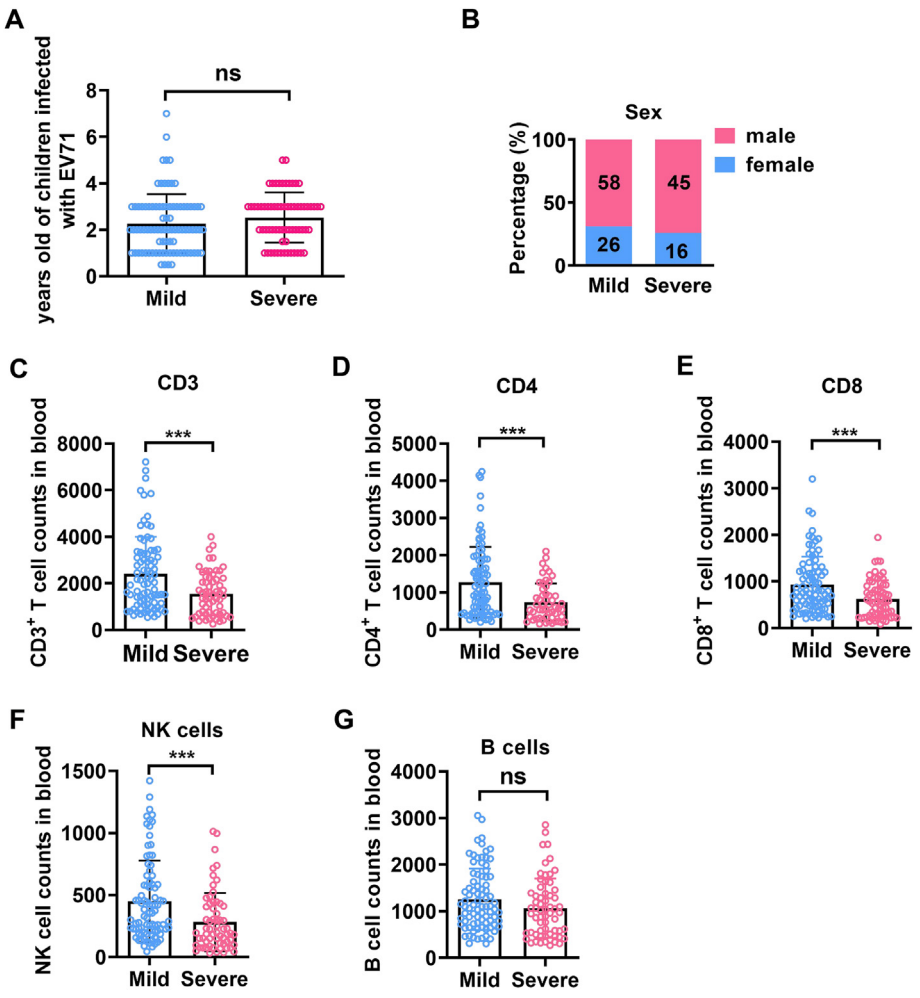

Fig. 4. Cohort study reveals the association of T-cell immunity with the severity of EV-A71-caused HFMDs in children. **(A, B)** The age (**A**) and gender (**B**) distribution of mild and severe HFMD patients with confirmed EV-A71 infection (n = 145). The X-axis represents different patient groups, and the Y-axis represents the age (**A**) or the ratio of genders (**B**). **C–G** The counts of $CD3^+CD45^+$ lymphocytes (**C**), $CD3^+CD4^+CD45^+$ lymphocytes (**D**), $CD3^+CD8^+CD45^+$ lymphocytes (**E**), $CD16^+CD56^+$ natural killer (NK) cells (**F**) and $CD19^+$ B cells (**G**) in the peripheral blood of HFMD patients with mild (n = 84) or severe (n = 61) clinical symptoms. Data are representative of three independent experiments. Graph shows mean ± SEM. *P* values were calculated via ANOVA. ***$P < 0.001$, ns, no significance.

results (Fig. 5B and Supplementary Fig. S4E–G). Therefore, these data show that AGS-A treatment has potent *in vivo* therapeutic efficacy against EV-A71 infection in newborn mice.

We sought to determine whether the action of AGS-A to treat EV-A71 infection in mice is associated with the immune response of T cells. Our data showed that although AGS-A treatment did not enhance the percentages of $CD3^+$ total T cells and $CD4^+$ T cells in spleens of non-infected 5-day-old ICR mice, it effectively restored the proportion of T cells to the same level as that in mice not infected with EV-A71 (Fig. 5C and D).

Activation of T cells requires the interaction of T cells with antigen-presenting cells via bi-molecular signals, including major histocompatibility complex (MHC) and CD86 (Xiaodong Feng and Administrative Sciences California Northstate University College of Pharmacy Rancho Cordova). Therefore, we assessed the effects of AGS-A on the expression levels of MHC-II and CD86 on $CD11b^+$ macrophages. And our data showed that AGS-A treatment significantly enhanced the expression of both MHC-II and CD86 (Fig. 5E–G). These results indicate that in the context of viral infection, AGS-A treatment can not only restore the immune response of T cells, but also activate T cells via stimulating bi-molecular signal expression on macrophages. Interestingly, AGS-A treatment failed to inhibit EV-A71 replication in rhabdomyosarcoma cells (RD cells) (Supplementary Fig. S5A), ruling out the possibility that AGS-A directly targets the life cycle of EV-A71. In addition, AGS-A showed minimal cytotoxicity (Supplementary Fig. S5B), further supporting the safety of AGS-A treatment.

Furthermore, we assessed whether the therapeutic effect of AGS-A is dependent on the presence of T cells. For this purpose, we also took the advantage of BALB/c-$nu^{-/-}$ mice that lack T cells, and examined the effects of AGS-A treatment on BALB/c-$nu^{-/-}$ mice challenged with EV-A71. Our data showed that although AGS-A treatment expectedly protected from EV-A71 infection in 5-day-old WT BALB/c mice (Fig. 6A–C), this saponin compound failed to show any therapeutic effects in the aspects of survival rate, body weights, and clinical scores, on the lethal EV-A71 challenge when being compared with non-treated, EV-A71-infected group in the 5-day-old BALB/c-$nu^{-/-}$ mice (Fig. 6D–F). These results show that the therapeutic effect of AGS-A is dependent on T cells.

In conclusion, our findings demonstrate that the therapeutic effect of AGS-A on the pathogenesis of EV-A71 infection in newborn mice is

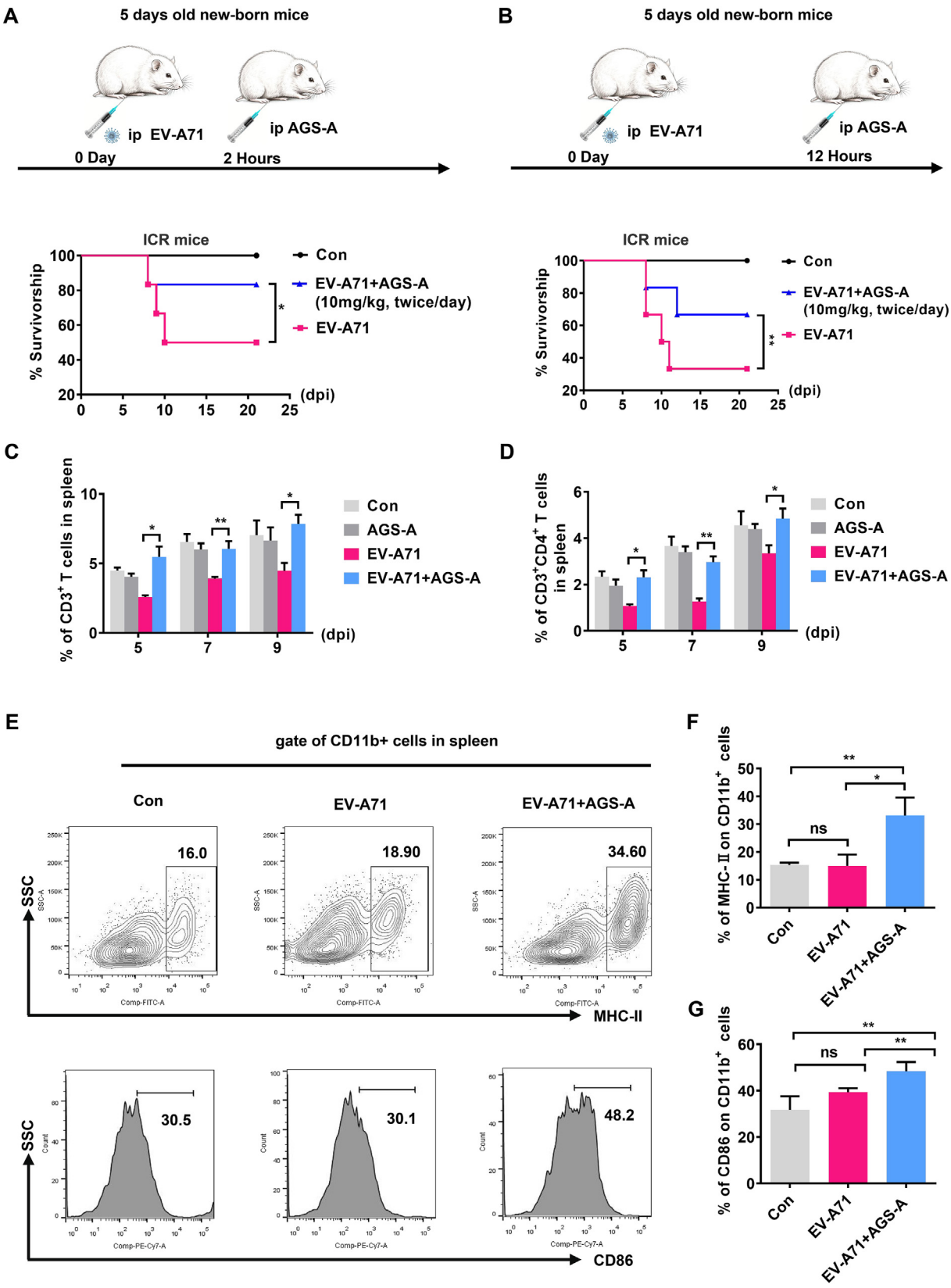

Fig. 5. AGS-A treatment protected from lethal EV-A71 infection by restoring the immune response of T cells. **A, B** 5-day-old ICR mice were treated with AGS-A (10 mg/kg) or PBS 2 h (**A**) or 12 h (**B**) after EV-A71 challenge, and control group were treated with PBS, followed by treatment twice a day for 6 days by i.p. administration. The survival rates for mice in different groups during the 21-day period are shown by curves. (n = 8 for each group). **C, D** The percentages of $CD3^+$ T (**C**) and $CD3^+CD4^+$ T cells (**D**) in the spleens of 5-day-old ICR mice in the indicated groups were determined by flow cytometry. **E–G** Representative scatter plots and bar charts showed the percentage of MHC-II (**E, F**) and CD86 (**E–G**) on $CD11b^+$ macrophages in the spleens of indicated mice. Data are representative of three independent experiments. Graph shows mean ± SEM. *P* values were calculated via ANOVA. $^*P < 0.05$, $^{**}P < 0.01$, ns, no significance.

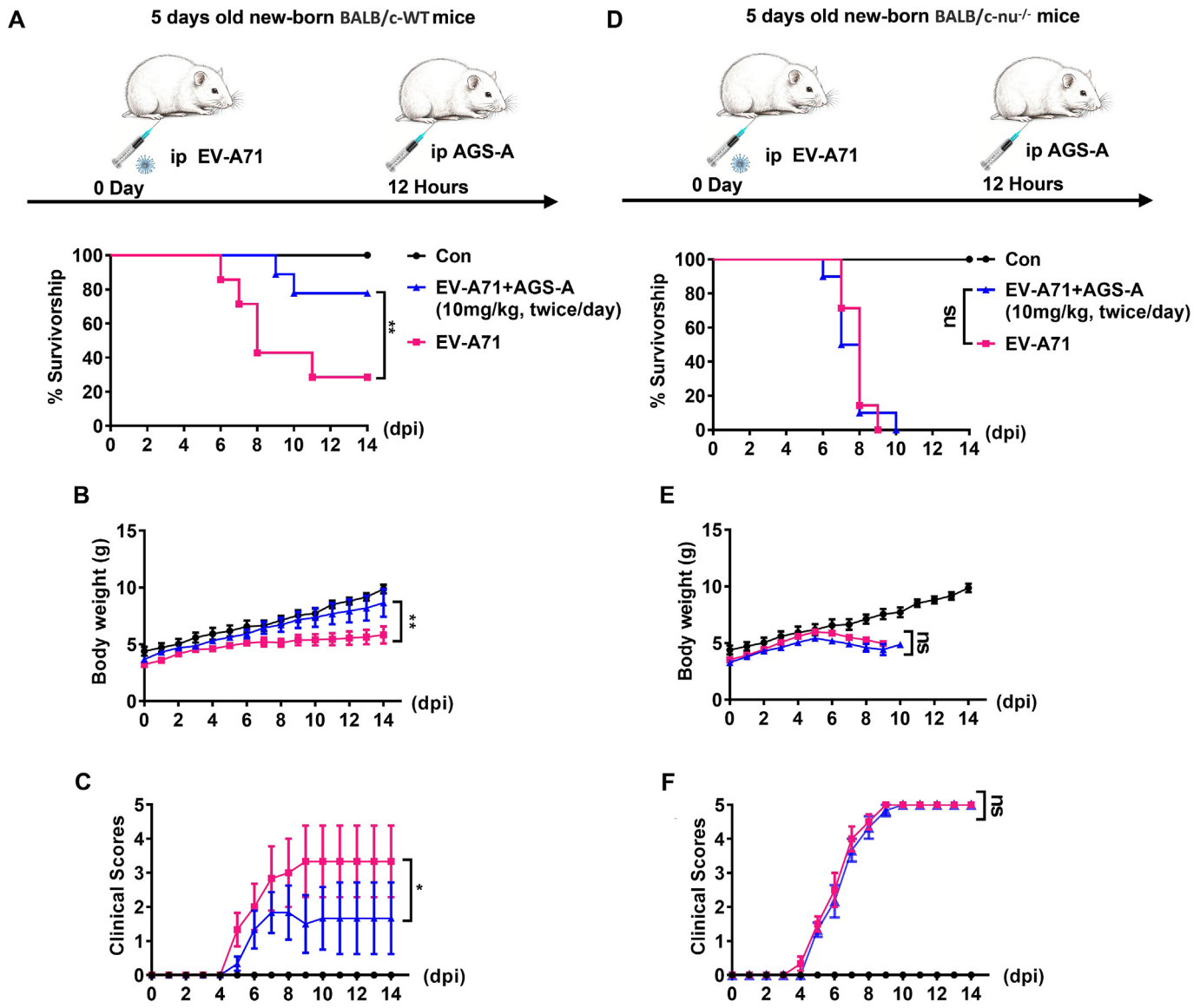

Fig. 6. AGS-A treatment protected from lethal EV-A71 infection only in mice with intact T-cell immunity. 5-day-old WT BABL/c **(A)** and BALB/c-nu$^{-/-}$ **(D)** mice were treated with 10 mg/kg AGS-A 12 h after EV-A71 challenge, followed by AGS-A treatment twice a day for 6 days. The survival rates of mice in the indicated groups during the 14-day period shown by curves. Body weights and clinical scores for the mice in **(A)** and **(D)** are plotted in **(B, C)** and **(E, F)**, respectively. Data are representative of three independent experiments. Graph shows mean ± SEM (n = 10). *P* values were calculated via ANOVA. $^{*}P < 0.05$, $^{**}P < 0.01$, ns, no significance.

T-cell-dependent, and AGS-A treatment has promising potential to be further developed as an immunotherapy for EV-A71 infection and HFMD in children.

DISCUSSION

HFMD caused by EV-A71 infection could be developed to severe symptoms and even lethality in young children under 5 years old, while the pathogenesis of severe HFMD is less understood. In the current study, we found that the underdevelopment of T-cell immune response was closely associated with the severity of EV-A71 infection in neonatal mice. Moreover, EV-A71 infection caused a dramatic impairment of T cell immune response in newborn mice, and the dysfunction of T cell immune response contributes to the pathogenesis of EV-A71 infection, as the loss of T cells made neonatal mice highly vulnerable to EV-A71 infection. Importantly, we further found that AGS-A could effectively rescue the EV-A71-caused impairment of T cell immune response, and showed potent *in vivo* therapeutic efficacy against EV-A71 infection in a T-cell-dependent manner in mouse model, implying that AGS-A treatment has promising potential to be developed as an immunotherapy for EV-A71 infection and HFMD.

Our study showed that the severe or lethal outcomes of EV-A71 infection only occurred in neonatal mice aged less than 2 weeks (Fig. 1B). Interestingly, we also uncovered that EV-A71 infection dramatically impaired T cell immune response in 3-day-old mice with immature T cell development, but not in 14-day-old mice with relatively well-developed T cells (Fig. 1C–E and Fig. 2). It is known that the adaptive immune system begins to mature at that time(Adkins et al., 2004), while T cells play important roles in the process of cellular immunity(Kumar et al., 2018; Lee et al., 2020; Mantovani et al., 2011). Moreover, our cohort study involving 145 pediatric patients who were laboratory-confirmed for EV-A71 infection and showed different HFMD symptoms ranging from mild to severe outcomes, further supported the notion that the disease severity of EV-A71 pediatric infection is closely associated with the dysfunction of T cell immune response in children, which is well in line with the *in vivo* data obtained using the infection murine model (Fig. 4). These findings are consistent with previous studies that cellular rather than humoral immunity is associated with the

clinical outcomes of EV-A71 infection(Chang et al., 2006, 2008; Lee et al., 2020; Shen et al., 2013; Yang et al., 2001). Therefore, the underdevelopment of T cells together with the EV-A71-caused impairment of T cell immune response should be the pivotal contributing factors for the pathogenesis of EV71 infection and HFMD.

AGS-A is a saponin extracted from *Astragalus membranaceus* (Lee et al., 2017) that has been used in traditional Chinese medicine for thousands of years to improve immune system. Modern medicinal researches on *Astragalus* have shown that it has great potential in immunomodulatory properties and antitumor activities (Li et al., 2014). Moreover, AGS-A was reported to inhibit tumor progression by downregulating the percentage of regulatory T cells and upregulating the percentage of cytotoxic T lymphocytes (Li et al., 2017). In addition, a recent study reported that AGS-IV inhibited EV-A71 replication in normal human gastric epithelial (GES-1) cells and RD cells via modulating PI3K-AKT signaling (Hao et al., 2024); however, we did not observe any direct anti-EV-A71 effect either in cells or in T-cell-deficient BALB/c-nu$^{-/-}$ mice infected with EV-A71, indicating that at least in the context of our experiments, the AGS-A conferred therapeutic effect on EV-A71 infection was associated with the effect of AGS-A on T cell response. In this study, our data showed that AGS-A treatment showed potent therapeutic effect to reduce the lethality and clinical symptoms of EV-A71 infection in a T-cell-dependent manner. Interestingly, such a treatment did not boost T cell immune response in the spleens of non-infected mice. The remaining, intriguing questions are how EV-A71 infection specifically impairs T cell immune response in neonatal mice but not in older ones with better developed T cells, and how AGS-A specifically restores such an impairment but not generally boosts T cell immunity. A possible explanation is that EV-A71 infection causes cell death in less matured T cells and/or induce certain cellular or signaling processes to inhibit T cells, while AGS-A treatment can reverse such effects. Answering these questions should further elucidate the pathogenesis of HFMD and reveal the mechanism of action of AGS-A in more details. Nevertheless, the rescuing but not general boosting effect of AGS-A on T cells makes this treatment less likely to induce excessive cellular immune response in recipients.

CONCLUSIONS

Our findings uncover the interaction between EV-A71 infection and T cell immunity, provide novel insights onto the physiological impacts of T cells on the pathogenesis of EV71 infection and HFMD, and find a promising immunotherapeutic strategy to treat this important pediatric infectious disease. Moreover, AGS-A, its derivatives as well as their different formulations should be further developed and assessed for their abilities as the treatment for EV-A71 infection and HFMD.

MATERIALS AND METHODS

Characterization of lymphocyte subsets in peripheral blood cells of children with EV-A71 infection

The EV-A71 group consisted of thirty-two cases of children with EV-A71 infection, who were admitted to Guangzhou Women and Children's Medical Center (Guangzhou, China) between November 2014 and July 2015. Pharyngeal swabs took from the children with the onset of fever within three days, rash in one or more parts of mouth, buttocks, hands or feet were examined for the presence of common pathogens by real-time reverse-transcription quantitative polymerase chain reaction (RT-qPCR) according to the protocols of the detection kits manufacturer (Daan Gene Co., Ltd of Sun Yat-Sen University, Shenzhen, China). All patients were confirmed with the diagnostic criteria of guideline for the diagnosis and treatment of HFMD (2018 Edition). Other common pathogens, including CV-A16, influenza virus, respiratory syncytial virus, adeno virus (ADV), human bocavirus, human metapneumovirus, parainfluenza virus (PIV), rhino virus (RHV), mycoplasma pneumoniae (MP), chlamydia pneumoniae, cytomegalovirus, Epsteine-Barr virus, and herpes simplex virus, were found negative in both groups. Informed consent was obtained from the legal parents of the children, and all procedures involved in this study were approved by the Ethics Committee of Guangzhou Women and Children's Medical Center.

Virus

The EV-A71 strain H (VR-1432) was obtained from ATCC, the virus was amplified and titers were determined in human rhabdomyosarcoma cells (RD cells) as previously described (Zhang et al., 2024). The virus was concentrated by ultrafiltration using Amicon Ultra-15 filters (Millipore) and quantified by plaque assay. Experiments including viral infections were conducted in Biosafety Level 2 (BSL-2) labs at Wuhan Institute of Virology.

Mice

Pathogen-free 18-day pregnant Institute of Cancer Research (ICR) mice, BALB/c mice, BALB/c-nu$^{-/-}$ mice were obtained from the animal housing facility of the Chinese Academy of Sciences (Changsha, China). All experiments were performed according to protocols approved by the Institutional Animal Care and Use Committee of Wuhan Institute of Virology.

Mice were i.p. injected with 10^7 PFU of EV-A71 in 50 μL of DMEM. Control animals received the same volume of DMEM via the same route. The time before infection was referred to as day 0. Infection with EV-A71 continued for day 10 to day 20 day, and mice presented clinical symptoms at 5 d.p.i. EV-A71-infected mice were sacrificed every other day up to day 9. A score was used to evaluate the clinical symptoms as previously described: 0, healthy; 1, hunchbacked and slow movement; 2, weakness in one limb; 3, paralysis in one limb; 4, paralysis in both limbs; and 5, death (He et al., 2018; Zhang et al., 2013).

The spleen of each mouse was collected and total RNAs from spleen were extracted with TRIzol (10296010) from Invitrogen. The viral RNA accumulation was determined via RT-qPCR with specific primers. The RT-qPCR was performed in a reaction mixture of Hieff® qPCR SYBR Green Master Mix (Low Rox Plus) (YEASEN), template, primers, reverse transcriptase (YEASEN) and RNase-free water. Primer sequences are available upon request and their sequences were listed in Supplementary Table S2.

Flow cytometry

Single-cell suspensions from the spleen and thymus were stained with different combinations of the following mAbs conjugated with FITC, PE, APC, PE-Cy7, and allophycocyanin as our previously described (Wang et al., 2017).

For cell surface maker staining, single-cell suspensions were incubated with the following Abs: FITC anti-CD3 (17A2; BioLegend), PE-Cy7 anti-CD4 (GK1.5; BioLegend), FITC anti-TCR-β (H57-597), PE anti-CD11c (N418; BioLegend), APC anti-CD11b (M1/70; BioLegend), PE anti-CD19 (6D5; BioLegend), PE-Cy7 anti-CD86 (GL-1; BioLegend) and FITC anti-IA/IE (M5/114.15.2) in 0.2% BSA (BioSharp) with PBS (pH 7.4) for 25 min at 4 °C. Cells were washed with PBS (400 g, 5 min, 4 °C) and fixed with 1% paraformaldehyde. Cells were determined using a FACS Calibur (BD Biosciences) system, and the data were analyzed using CellQuest Pro software (BD Biosciences).

AGS-A treatment

AGS-A (83207-58-3) were commercially purchased from Selleck. 5-day-old ICR mice were treated with AGS-A at the dose of 10 mg/kg within vehicle 2 h or 12 h after challenge with EV-A71, followed by treatment twice a day or once a day for 6 days by i.p. administration. 10-day-old BALB/c-nu$^{-/-}$ mice were treated with Astragal side at the dose of

10 mg/kg within vehicle 12 h after challenge with EV-A71, followed by treatment twice a day or once a day for 6 days by i.p. injection. The survival distribution for mice during the 21-d period is shown by curves.

Cell culture and virus infection

The RD cell line was commercially obtained from ATCC and maintained in Dulbecco's modified Eagle's medium (DMEM, Gibco) supplemented with 10% fetal bovine serum (Gibco), 100 U/mL penicillin and 100 μg/mL streptomycin at 37 °C in a humidified atmosphere with 5% CO_2. The EV-A71 strain VR-1432 were obtained from ATCC.

The CCK-8 assay was used to evaluate the cytotoxicity of AGS-A in RD cells. Briefly, the cells were seeded into 96-well plates and incubated with increased concentrations from 0 μM to 1280 μM. After incubation at 37 °C for 12 h, the cell supernatant was replaced with fresh DMEM. Then, after incubation for additional 12 h, the CCK-8 solution was added for detection of the absorbance at 450 nm using a microplate reader (Infinite M200PRO). The CCK-8 kit was purchased from Dojindo.

For detection of the effects of AGS-A on EV-A71 infection, each one of the tested compounds at the concentration of 5 or 10 μM was added to RD cells (4×10^5 cells in each of the 12 wells in a cell culture-treated plate). After 1 h incubation, RD cells were infected with EV-A71 at MOI = 0.1. At 12 h post-infection, the infected RD cells were collected and total cellular RNAs were extracted using Total RNA kit (Foregene). The viral RNA accumulation was determined via qRT-PCR. The qRT-PCR was performed using One Step SYBR® PrimeScript™ PLUS RT-PCR Kit (Yeasen). All the primers used here are listed in Supplementary Table S2.

Statistical analyses

All data were analyzed with GraphPad Prism (GraphPad Software, La Jolla, CA). Data are expressed as the mean SEM, and the significance of differences between groups was evaluated by using a parametric ANOVA test. A *P*-value of 0.05 was considered significant.

DATA AVAILABILITY

All data relevant to the study are included in the article or uploaded as supplementary information.

ETHICS STATEMENT

All animal research protocols strictly adhere to the Guidelines for the Care and Use of Laboratory Animals at the Wuhan Institute of Virology, Chinese Academy of Sciences (CAS). All experiments comply with relevant regulatory standards. The experiments and protocols have been approved by the Ethics Committee of the Wuhan Institute of Virology (WIVA24202005). All human - sourced materials were obtained in strict accordance with the 'Ethical Guidelines for the Acquisition and Use of Human - sourced Materials' at the Guangzhou Women and Children's Medical Center. All procedures comply with relevant regulatory requirements. The acquisition of human - sourced materials and related protocols have been approved by the Ethics Committee of the Guangzhou Women and Children's Medical Center (Approval No. 250A01).

AUTHOR CONTRIBUTIONS

Chong Wang performed most experiments. Muhan Huang and Bingyu Guo performed specific experiments. Yi Xu and Yujie Ren conceived the idea. Chong Wang, Zongqiang Cui, Yi Xu, and Xi Zhou designed the experiments and analyzed the data. Chong Wang, Zongqiang Cui, and Yujie Ren wrote the manuscript with the inputs from all authors. Yi Xu and Yujie Ren supervised the study.

CONFLICT OF INTEREST

Prof. Zongqiang Cui and Prof. Xi Zhou are editorial board members for *Virologica Sinica* and were not involved in the editorial review or the decision to publish this article. The authors declare no competing interest.

ACKNOWLEDGEMENTS

This work was supported by the National Natural Science Foundation of China (32200130 to Chong Wang and 82372228 to Yi Xu), the 2023–2024 Annual Scientific Research Project of Traditional Chinese Medicine from Hubei Provincial Administration of Traditional Chinese Medicine (ZY2023Q050 to Chong Wang), and Hubei Province Natural Science Funds (2023AFA008 to Xi Zhou).

APPENDIX A. SUPPLEMENTARY DATA

Supplementary data to this article can be found online at https://doi.org/10.1016/j.virs.2025.05.010.

REFERENCES

Adkins, B., Leclerc, C., Marshall-Clarke, S., 2004. Neonatal adaptive immunity comes of age. Nat. Rev. Immunol. 4, 553–564.
Auyeung, K.K., Han, Q.B., Ko, J.K., 2016. Astragalus membranaceus: a review of its protection against inflammation and gastrointestinal cancers. Am. J. Chin. Med. 44, 1–22.
Carsetti, R., Quintarelli, C., Quinti, I., Piano Mortari, E., Zumla, A., Ippolito, G., Locatelli, F., 2020. The immune system of children: the key to understanding SARS-CoV-2 susceptibility? Lancet Child Adolesc. Health 4, 414–416.
Chan, L.G., Parashar, U.D., Lye, M.S., Ong, F.G., Zaki, S.R., Alexander, J.P., Ho, K.K., Han, L.L., Pallansch, M.A., Suleiman, A.B., Jegathesan, M., Anderson, L.J., 2000. Deaths of children during an outbreak of hand, foot, and mouth disease in sarawak, Malaysia: clinical and pathological characteristics of the disease. For the outbreak study group. Clin. Infect. Dis. 31, 678–683.
Chang, L.Y., Hsiung, C.A., Lu, C.Y., Lin, T.Y., Huang, F.Y., Lai, Y.H., Chiang, Y.P., Chiang, B.L., Lee, C.Y., Huang, L.M., 2006. Status of cellular rather than humoral immunity is correlated with clinical outcome of enterovirus 71. Pediatr. Res. 60, 466–471.
Chang, L.Y., Chang, I.S., Chen, W.J., Huang, Y.C., Chen, G.W., Shih, S.R., Juang, J.L., Shih, H.M., Hsiung, C.A., Lin, T.Y., Huang, L.M., 2008. HLA-A33 is associated with susceptibility to enterovirus 71 infection. Pediatrics 122, 1271–1276.
Deng, C., Yang, C., Wan, J., Zhu, L., Leng, Q., 2011. Irregular poliovirus vaccination correlates to pulmonary edema of hand, foot, and mouth disease. Clin. Vaccine Immunol. 18, 1589–1590.
Fioravanti, C.H., 2012. Brazilian fitness programme registers health benefits. Lancet 380, 206.
Hao, J., Zhang, X., Hu, R., Lu, X., Wang, H., Li, Y., Cheng, K., Li, Q., 2024. Metabolomics combined with network pharmacology reveals a role for astragaloside IV in inhibiting enterovirus 71 replication via PI3K-AKT signaling. J. Transl. Med. 22, 555.
He, Q.Q., Ren, S., Xia, Z.C., Cheng, Z.K., Peng, N.F., Zhu, Y., 2018. Fibronectin facilitates enterovirus 71 infection by mediating viral entry. J. Virol. 92, e02251-17.
Ho, M., Chen, E.R., Hsu, K.H., Twu, S.J., Chen, K.T., Tsai, S.F., Wang, J.R., Shih, S.R., 1999. An epidemic of enterovirus 71 infection in taiwan. Taiwan enterovirus epidemic working group. N. Engl. J. Med. 341, 929–935.
Huang, C.C., Liu, C.C., Chang, Y.C., Chen, C.Y., Wang, S.T., Yeh, T.F., 1999. Neurologic complications in children with enterovirus 71 infection. N. Engl. J. Med. 341, 936–942.
Kumar, B.V., Connors, T.J., Farber, D.L., 2018. Human T cell development, localization, and function throughout life. Immunity (Camb., Mass.) 48, 202–213.
Lee, S.Y., Tsai, W.C., Lin, J.C., Ahmetaj-Shala, B., Huang, S.F., Chang, W.L., Chang, T.C., 2017. Astragaloside II promotes intestinal epithelial repair by enhancing L-arginine uptake and activating the mTOR pathway. Sci. Rep. 7, 12302.
Lee, H.G., Cho, M.Z., Choi, J.M., 2020. Bystander CD4(+) T cells: crossroads between innate and adaptive immunity. Exp. Mol. Med. 52, 1255–1263.
Li, X., Qu, L., Dong, Y., Han, L., Liu, E., Fang, S., Zhang, Y., Wang, T., 2014. A review of recent research progress on the astragalus genus. Molecules (Basel) 19, 18850–18880.
Li, L., Hou, X., Xu, R., Liu, C., Tu, M., 2017. Research review on the pharmacological effects of astragaloside IV. Fundam. Clin. Pharmacol. 31, 17–36.
Mantovani, A., Cassatella, M.A., Costantini, C., Jaillon, S., 2011. Neutrophils in the activation and regulation of innate and adaptive immunity. Nat. Rev. Immunol. 11, 519–531.
Olin, A., Henckel, E., Chen, Y., Lakshmikanth, T., Pou, C., Mikes, J., Gustafsson, A., Bernhardsson, A.K., Zhang, C., Bohlin, K., Brodin, P., 2018. Stereotypic immune system development in newborn children. Cell 174, 1277–1292.

Pallansch, M.A., 2007. In: Virology, Fields, Knipe, D.M.H., Peter, M. (Eds.), Enteroviruses: Polioviruses, Coxsackieviruses, Echoviruses, and Newer Enteroviruses. Lippioncott Williams & Wilkonson, Philadelphia, pp. 840–893.

Shen, F.-H., Tsai, C.-C., Wang, L.-C., Chang, K.-C., Tung, Y.-Y., Su, I.-J., Chen, S.-H., 2013. Enterovirus 71 infection increases expression of interferon-gamma-inducible protein 10 which protects mice by reducing viral burden in multiple tissues. J. Gen. Virol. 94, 1019–1027.

Simon, A.K., Hollander, G.A., McMichael, A., 2015. Evolution of the immune system in humans from infancy to old age. Proc. Biol. Sci. 282, 20143085.

Solomon, T., Lewthwaite, P., Perera, D., Cardosa, M.J., McMinn, P., Ooi, M.H., 2010. Virology, epidemiology, pathogenesis, and control of enterovirus 71. Lancet Infect. Dis. 10, 778–790.

Tan, X., Huang, X., Zhu, S., Chen, H., Yu, Q., Wang, H., Huo, X., Zhou, J., Wu, Y., Yan, D., Zhang, Y., Wang, D., Cui, A., An, H., Xu, W., 2011. The persistent circulation of enterovirus 71 in People's Republic of China: causing emerging nationwide epidemics since 2008. PLoS One 6, e25662.

Wang, C., Zhang, N., Qi, L., Yuan, J., Wang, K., Wang, K., Ma, S., Wang, H., Lou, W., Hu, P., Awais, M., Cao, S., Fu, Z.F., Cui, M., 2017. Myeloid-derived suppressor cells inhibit T follicular helper cell immune response in Japanese encephalitis virus infection. J. Immunol. 199, 3094–3105.

Yang, K.D., Yang, M.Y., Li, C.C., Lin, S.F., Chong, M.C., Wang, C.L., Chen, R.F., Lin, T.Y., 2001. Altered cellular but not humoral reactions in children with complicated enterovirus 71 infections in Taiwan. J. Infect. Dis. 183, 850–856.

Zhang, Q.Y., Li, J.Q., Li, Q., Zhang, Y., Zhang, Z.R., Li, X.D., Zhang, H.Q., Deng, C.L., Yang, F.X., Xu, Y., Zhang, B., 2024. Identification of fangchinoline as a broad-spectrum enterovirus inhibitor through reporter virus based high-content screening. Virol. Sin. 39, 301–308.

Zhang, X., Song, Z., Qin, B., Zhang, X., Chen, L., Hu, Y., Yuan, Z., 2013. Rupintrivir is a promising candidate for treating severe cases of enterovirus-71 infection: evaluation of antiviral efficacy in a murine infection model. Antivir. Res. 97, 264–269.

Zhu, K., Yang, J., Luo, K., Yang, C., Zhang, N., Xu, R., Chen, J., Jin, M., Xu, B., Guo, N., Wang, J., Chen, Z., Cui, Y., Zhao, H., Wang, Y., Deng, C., Bai, L., Ge, B., Qin, C.F., Shen, H., Yang, C.-F., Leng, Q., 2015. TLR3 signaling in macrophages is indispensable for the protective immunity of invariant natural killer T cells against enterovirus 71 infection. PLoS Pathog. 11, e1004613.